

# Mechanism of Insolubilization by a Single-Point Mutation in $\alpha$ A-Crystallin Linked with Hereditary Human Cataracts<sup>†</sup>

Usha P. Andley,<sup>\*,‡,§</sup> Paul D. Hamilton,<sup>‡,||</sup> and Nathan Ravi<sup>‡,||</sup>

Department of Ophthalmology and Visual Sciences and Department of Biochemistry and Molecular Biophysics, Washington University School of Medicine, St. Louis, Missouri 63110, and Research, Veterans Administration Medical Center, St. Louis, Missouri 63106

Received April 4, 2008; Revised Manuscript Received June 12, 2008

**ABSTRACT:**  $\alpha$ A-Crystallin is a small heat shock protein that functions as a molecular chaperone and a lens structural protein. The R49C single-point mutation in  $\alpha$ A-crystallin causes hereditary human cataracts. We have previously investigated the *in vivo* properties of this mutant in a gene knock-in mouse model. Remarkably, homozygous mice carrying the  $\alpha$ A-R49C mutant exhibit nearly complete lens opacity concurrent with small lenses and small eyes. Here we have investigated the 90° light scattering, viscosity, refractive index, and bis-ANS fluorescence of lens proteins isolated from the  $\alpha$ A-R49C mouse lenses and found that the concentration of total water-soluble proteins showed a pronounced decrease in  $\alpha$ A-R49C homozygous lenses. Light scattering measurements on proteins separated by gel permeation chromatography showed a small amount of high-molecular mass aggregated material in the void volume which still remains soluble in  $\alpha$ A-R49C homozygous lens homogenates. An increased level of binding of  $\beta$ - and  $\gamma$ -crystallin to the  $\alpha$ -crystallin fraction was observed in  $\alpha$ A-R49C heterozygous and homozygous lenses but not in wild-type lenses. Quantitative analysis with the hydrophobic fluorescence probe bis-ANS showed a pronounced increase in fluorescence yield upon binding to  $\alpha$ -crystallin from mutant as compared with the wild-type lenses. These results suggest that the decrease in the solubility of the  $\alpha$ A-R49C mutant protein was due to an increase in its hydrophobicity and supra-aggregation of  $\alpha$ A-crystallin that leads to cataract formation. Our study further shows that analysis of mutant proteins from the mouse model is an effective way to understand the mechanism of protein insolubilization in hereditary cataracts.

Small heat shock proteins are defined by their 15–30 kDa subunit mass and a highly conserved “ $\alpha$ -crystallin” domain of approximately 90 amino acids in their C-terminal region (1, 2). These proteins have recently received significant attention due to their involvement in diverse human pathologies, including neurological diseases and hereditary cataracts (3–6). Two members of this family,  $\alpha$ A- and  $\alpha$ B-crystallin, accumulate to very high concentrations in lens fiber cells and are present in a 3:1 stoichiometry (7). Both  $\alpha$ A- and  $\alpha$ B-crystallin function as molecular chaperones and prevent nonspecific aggregation of denaturing proteins *in vitro* (8, 9).  $\alpha$ A-Crystallin is expressed in only a small number of tissues outside the lens, whereas  $\alpha$ B-crystallin is widely distributed and is upregulated under a variety of stress conditions (5). Targeted gene deletion studies of  $\alpha$ A-crystallin,  $\alpha$ B-crystallin, or both proteins in mice have

provided significant information about their roles in preserving lens transparency, growth, and development (3, 10–13).

The transparency of the human eye lens depends on the properties of the crystallins which are expressed at very high concentrations in lens fiber cells. The subunit mass of  $\alpha$ A- and  $\alpha$ B-crystallin is approximately 20 kDa, and their amino acid sequences are 57% identical.  $\alpha$ A-Crystallin comprises nearly 20% of the total water-soluble protein in newborn human lenses (14, 15). While the  $\alpha$ -crystallins form oligomeric aggregates varying in molecular mass from 600 kDa to 1.2 MDa in lens fiber cells, these cells also express an abundance of another class of crystallins,  $\beta\gamma$ . The  $\beta$ -crystallins form smaller oligomers (60–180 kDa), whereas  $\gamma$ -crystallins are monomeric polypeptides with molecular masses of ~20 kDa (16, 17). Aggregation and insolubilization of crystallins are considered major causes of formation of age-related and hereditary human cataracts (18, 19). Age-related modifications in  $\alpha$ -crystallin have been shown to increase the level of formation of water-soluble high-molecular mass protein aggregates which eventually become insoluble (20, 21). The increase in protein aggregate size is directly responsible for an increase in light scattering and lens opacification. A decrease in protein solubility has also been reported with several cataract-causing point mutations in  $\gamma$ -crystallins (22–24).

In recent years, a number of point mutations have been discovered in the genes for  $\alpha$ A- and  $\alpha$ B-crystallin that cause

<sup>†</sup> This work is supported by NIH Grant EY05681 to U.P.A., Core Grant EY02687, an unrestricted grant to the Department of Ophthalmology and Visual Sciences of Washington University from RPB, and a VA Merit Review Grant to N.R.

\* To whom correspondence should be addressed: Washington University School of Medicine, 660 S. Euclid Ave., Campus Box 8096, St. Louis, MO 63110. Fax: (314) 362-3638. E-mail: andley@vision.wustl.edu.

<sup>‡</sup> Department of Ophthalmology and Visual Sciences, Washington University School of Medicine.

<sup>§</sup> Department of Biochemistry and Molecular Biophysics, Washington University School of Medicine.

<sup>||</sup> Veterans Administration Medical Center.

hereditary human cataracts (6). Point mutations in  $\alpha$ A-crystallin (R116C, R49C, and G98R) have been shown to cause human hereditary cataracts, and the R120G and D140N mutations in  $\alpha$ B-crystallin cause desmin-related myopathy and/or hereditary human cataracts (4, 25–28). The mechanisms that lead to cataract formation as a result of these mutations are not fully understood. Among these mutations, only the R49C mutation in  $\alpha$ A-crystallin lies outside the conserved  $\alpha$ -crystallin domain of the small heat shock proteins. The N-terminal region has been shown to be important in oligomeric assembly of  $\alpha$ -crystallin (29–31). An increased level of exposure of the N-terminal region in small heat shock protein Hsp16.5 correlates with enhanced substrate binding of destabilized substrates, suggesting that this region is important in determining the solubility of the  $\alpha$ -crystallin oligomeric complex (32, 33). However, the mechanism by which  $\alpha$ -crystallin becomes insoluble is poorly understood.

The size, morphology, and temporal process of lens opacification in human patients with the arginine 49 to cysteine ( $\alpha$ A-R49C)<sup>1</sup> mutation are unknown at present. The effects of the R49C mutation in  $\alpha$ A-crystallin have been investigated in cultured cells, and the mutation is known to enhance lens epithelial cell death, cause the mislocalization of  $\alpha$ A-crystallin from the cytoplasm into the cellular nucleus, and diminish the resistance of cells to stress conditions (26). To understand how this point mutation in  $\alpha$ A-crystallin affects the lens in vivo, our laboratory recently generated a knock-in mouse model for hereditary human cataracts caused by the R49C mutation in  $\alpha$ A-crystallin (34). The advantage of this mouse model over in vitro expression of the mutant protein is that it replicates the heterozygosity of the human pathology in vivo. This model also allows the testing of gene dosing effects via analyses of lens changes in heterozygous and homozygous mice. We reported that  $\alpha$ A-R49C heterozygosity causes protein insolubility and lens opacities that were apparent at an early postnatal age.  $\alpha$ A-R49C homozygosity enhances protein insolubility and lens cell death in vivo, leading to a small eye, small lens, and severe cataracts at birth (34). The mechanism by which  $\alpha$ A-R49C becomes insoluble is not known. This report investigated the consequence of the mutation on protein insolubility by measuring the light scattering, refractive index, and viscosity of proteins separated by gel permeation chromatography, in conjunction with analysis of hydrophobicity using the fluorescent probe bis-ANS. We demonstrate here that protein insolubility in  $\alpha$ A-R49C lenses is likely to be the result of an increase in the hydrophobicity of  $\alpha$ -crystallin and an increase in the level of binding of  $\beta$ - and  $\gamma$ -crystallins to  $\alpha$ -crystallin in the mutant lenses.

## MATERIALS AND METHODS

**Animals and Lenses.** Knock-in mice expressing the C to T single-point mutation in codon 49 of the mouse  $\alpha$ A-crystallin gene (*cryaa*) resulting in the substitution of arginine 49 with cysteine (R49C) were generated by methods

described previously (34). Briefly, a knock-in plasmid was generated by cloning the 5' and 3' arms of the mouse  $\alpha$ A-crystallin gene, followed by mutation and homologous recombination in mouse embryonic stem cells, which were implanted into mice to generate the  $\alpha$ A-R49C knock-in mice. Heterozygous  $\alpha$ A-R49C mice expressed one copy of the mutant gene, while the second copy was the wild type. Homozygous mice containing two copies of the mutant gene were generated by interbreeding of heterozygous mice. Wild-type littermates were used as controls. Mice used in this study were from the 129 Sv strain backcrossed with the C57BL6 strain for several generations. PCR-based screening was routinely used to genotype the animals. Mice were maintained at Washington University by the Division of Comparative Medicine by trained veterinary staff. All protocols and procedures involving animals were approved by the Animal Studies Committee. Mice were euthanized using CO<sub>2</sub> inhalation, and lenses were dissected from 3–6-month-old mice.

**Preparation of Samples for Gel Chromatography.** For each chromatographic run, four mouse lenses (3–6 months old) were used to isolate water-soluble proteins from wild-type and  $\alpha$ A-R49C heterozygous mouse eyes, but because of their smaller size, 12 lenses were used from  $\alpha$ A-R49C homozygous mice. Lenses were homogenized in 50 mM Tris-HCl (pH 7.4) containing 100 mM NaCl, 1 mM DTT, and 1 mM EDTA, and the water-soluble protein fraction was separated by centrifugation at 15000g.

**Analytical Chromatography and Analysis.** HPLC gel filtration chromatography (GPC) was performed using a Spectraseries P200 pump (Thermo Separation Products, Waltham, MA) with a MetaChem (Torrance, CA) degasser equipped with triple detectors (Viscotek Corp., Houston, TX) that measured the refractive index (RI), right angle laser light scattering, and viscosity, supplemented with an additional UV Waters 490E detector set at 280 nm (Waters Corp., Milford, MA). Two columns were connected in series, an A4000PWXL column and a G4000PWXL column (Tosoh Biosep, Montgomeryville, PA). Viscotek Trisec (Viscotek Corp.) was used to calculate the RI area, weight-average molecular mass, intrinsic viscosity, and radius of gyration. Samples were injected at various volumes and concentrations. The flow rate was 0.8 mL/min, and the column buffer was comprised of 50 mM Tris, 100 mM NaCl, 1 mM EDTA, 1 mM DTT, and 0.1% NaN<sub>3</sub> (pH 7.5). Samples from the column were collected for further analysis as follows. The amounts of protein present in the wild-type  $\alpha$ A-crystallin,  $\alpha$ A-R49C heterozygous, and  $\alpha$ A-R49C homozygous lens samples were calculated using refractive index (RI) area. Samples from each condition were then run using approximately equal amounts of total protein. Column fractions for each condition were collected at 1 min intervals (800  $\mu$ L/tube).

**Molecular Mass Standards.** Protein standards with known molecular mass were used to standardize the column and the detectors. Identical conditions were then used for the separation of lens crystallins. Molecular mass protein standards were obtained from Amersham Biosciences (GE Healthcare, Piscataway, NJ). The high-molecular mass protein standards were dextran blue (2000 kDa), thyroglobulin (669 kDa), catalase (232 kDa), and aldolase (158 kDa). The low-molecular mass protein standards were bovine

<sup>1</sup> Abbreviations:  $\alpha$ A-R49C, arginine to cysteine mutation in  $\alpha$ A-crystallin; bis-ANS, 1,1'-bis(4-anilino)naphthalene-5,5'-disulfonic acid; DTT, dithiothreitol; HRP, horseradish peroxidase; IgG, immunoglobulin; SDS-PAGE, sodium dodecyl sulfate-polyacrylamide gel electrophoresis.

serum albumin (67 kDa), chymotrypsin (25 kDa), and ribonuclease A (13.7 kDa).

**Determination of Molecular Mass from Light Scattering and Refractive Index.** Using static light scattering as the analytical tool, we determined the change in the weight-average molecular mass of water-soluble  $\alpha$ -crystallin isolated from wild-type,  $\alpha$ A-R49C heterozygous, and  $\alpha$ A-R49C homozygous mutant mouse lenses. In this modality, the frequency of the scattered light is the same as that of the incoming light and samples scatterers in the spatial domain as the light beam encounters their refractive index fluctuations along its optical pathway (18). The viscosity measurement is used to calculate the radius of gyration of the  $\alpha$ -crystallin aggregate. Light scattering data were collected over a range of protein concentrations. Viscotek Trisec (Viscotek Corp.) was used to calculate the refractive index (RI) area, weight-average molecular mass, intrinsic viscosity, and radius of gyration. The software uses an angular correction calculation in determining molecular masses. This method has been adapted from the Trisec GPC software handbook (Viscotek Corp.).

**Fluorescence Measurements.** Fluorescence measurements were taken with a Perkin-Elmer LS50 spectrofluorometer with a FLWinlab data station. The concentration of the protein was 0.1 mg/mL (approximately 0.125  $\mu$ M). The protein concentration was determined using an  $A^{0.1\%}$  of 0.742. The excitation and emission slits were set to 5 nm. Samples with 4,4'-dianilino-1,1'-binaphthalene-5,5'-disulfonic acid (bis-ANS) were excited at 360 nm, and fluorescence emission was measured between 400 and 600 nm in a cuvette with a path length of 1 cm at a scan rate of 100 nm/min. Bis-ANS (1–5  $\mu$ M) was either scanned alone in buffer or added to the  $\alpha$ -crystallin fraction from the gel permeation chromatography column. All measurements were taken at 25 °C.

**Thermal Stability.** Time-dependent changes in the light scattering of water-soluble protein fractions from wild-type, heterozygous, and homozygous lenses were measured by heating to 65 °C. Light scattering was measured in a spectrofluorometer set at excitation and emission wavelengths of 360 nm. Temperature-induced stability of protein solutions was also measured by heating them to different temperatures (25, 37, 42, 53, and 65 °C) for 30 min and measuring the light scattering intensity at 360 nm (9, 28).

**Immunoblot Analysis of Gel Permeation Chromatography Fractions.** Mouse lens crystallin fractions, harvested from gel permeation chromatography columns, were mixed with 30  $\mu$ L of SDS–PAGE sample buffer (5 $\times$ ) containing 0.02 M Tris-HCl (pH 6.8), 4%  $\beta$ -mercaptoethanol, 4 mg/mL bromophenol blue, 5% SDS, and 60% glycerol. A 15  $\mu$ L aliquot was analyzed by SDS–PAGE using 15% gels. Proteins were transferred to PVDF membranes and probed with primary antibodies to  $\alpha$ A-crystallin (a monoclonal antibody to bovine  $\alpha$ A-crystallin used at a 1:40 dilution) (10), and polyclonal antibodies to the total bovine  $\alpha$ -crystallin,  $\beta$ -crystallin, and  $\gamma$ -crystallin used at a 1:2000 dilution (35, 36). The secondary antibodies were HRP-labeled anti-mouse or HRP-labeled anti-rabbit IgGs. Blots were incubated with luminol reagent (Santa Cruz Biotechnology) and exposed to Kodak film to visualize the protein bands. In these analyses, crystallins isolated by gel permeation chromatography from human lenses were used as controls.

## RESULTS

The  $\alpha$ A-R49C mutant is associated with cataracts. We have generated knock-in mice expressing the  $\alpha$ A-R49C heterozygosity of human patients as well as  $\alpha$ A-R49C homozygous mice and analyzed their lens proteins. To determine the effect of the mutation on the molecular mass of the  $\alpha$ -crystallin aggregate, gel permeation chromatography of the water-soluble proteins from wild-type,  $\alpha$ A-R49C heterozygous, and  $\alpha$ A-R49C homozygous mouse lenses was performed. Figure 1 shows the chromatography profile for wild-type water-soluble lens proteins measured by viscosity, light scattering, and refractive index.  $\alpha$ -,  $\beta$ H ( $\beta$ -heavy)-,  $\beta$ L ( $\beta$ -light)-, and  $\gamma$ -crystallin lens protein fractions showed an excellent separation based upon the differences in the refractive indexes of these proteins.  $\alpha$ -Crystallin is the major contributor to light scattering. The viscosity curve parallels the refractive index profile of the proteins and further shows a small peak in the protein fractions eluting in the void volume of the column. Table 1 shows the effect of the  $\alpha$ A-R49C mutation on the protein concentration of the water-soluble lens fraction. The protein concentration of the water-soluble fraction of the  $\alpha$ A-R49C knock-in mouse lens proteins decreased by 20% in heterozygous lenses and by 84% in homozygous lenses compared with wild-type proteins (6.0 mg/mL for wild-type, 4.8 mg/mL for heterozygous, and 1 mg/mL for homozygous mouse lenses). The average of at least two pooled lenses from two different preparations for each genotype is shown. The significantly lower degree of insolubilization in heterozygous knock-in mouse lenses that express both the wild-type and mutant  $\alpha$ A-crystallin suggests that the presence of wild-type  $\alpha$ A-crystallin protects against protein insolubility. Furthermore, comparison of the light scattering profiles showed that  $\alpha$ A-R49C homozygous lenses demonstrate a peak in the void volume corresponding to aggregates of proteins of  $\geq 2$  MDa (Figure 2). Analysis of the water-soluble proteins of  $\alpha$ A-R49C homozygous lenses by gel permeation chromatography showed a loss of the  $\beta$ L fraction from the soluble phase of the  $\alpha$ A-R49C homozygous lenses (Figure 3A). Figure 3B shows a plot of the molecular masses of protein fractions obtained from the gel permeation chromatography column. A new low-molecular mass 15 kDa protein (Figure 3B, arrow) and loss of an  $\sim 60$  kDa protein (Figure 3B, arrowhead) were observed in the homozygous lenses. The weight-average molecular masses of the major peaks were not significantly different among the three genotypes, but the greatly reduced protein concentration (Table 1) in the homozygous lenses suggests that the formation of water-insoluble high-molecular mass aggregated proteins is the major effect of the mutation. Table 2 shows the weight-average molecular masses, viscosities, and radii of gyration of the major protein peaks obtained by gel permeation chromatography of the water-soluble lens proteins. The UV chromatogram of the water-soluble lens proteins also clearly demonstrated a loss of the  $\beta$ L- and  $\gamma$ -crystallin peak in  $\alpha$ A-R49C homozygous lenses (Figure 4A). A comparison of the results in Figures 3A and 4A suggests that the refractive index detector separated the  $\beta$ L- and  $\gamma$ -crystallins much better than the UV detector. The identity of the protein peak fractions separated by gel permeation chromatography was confirmed by immunoblot analysis with antibodies specific to bovine  $\alpha$ -,  $\beta$ -, and



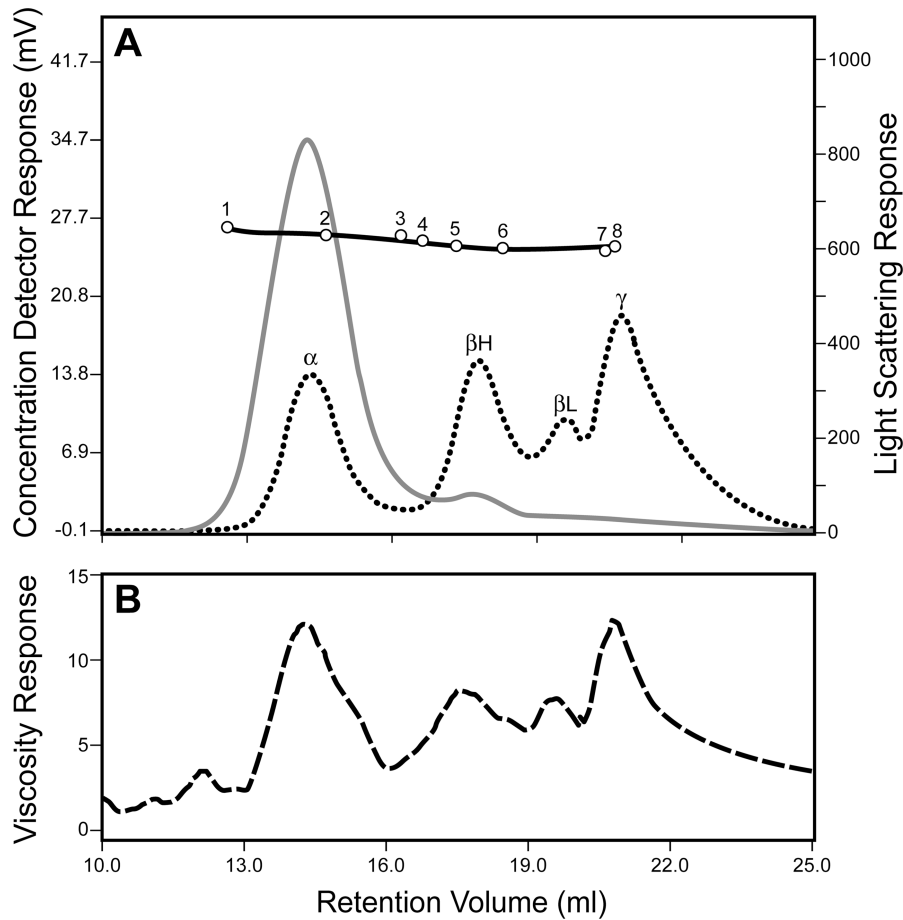


FIGURE 1: Gel permeation profile of lens proteins from wild-type mouse lenses. (A) Light scattering (solid gray line) and refractive index (dotted black line) measurements on proteins eluting from the column. The column was calibrated using molecular mass markers (1) dextran blue (2 MDa), (2) thyroglobulin (669 kDa), (3) ferritin (440 kDa), (4) catalase (232 kDa), (5) aldolase (156 kDa), (6) bovine serum albumin (67 kDa), (7) chymotrypsin (25 kDa), and (8) ribonuclease A (12.5 kDa). (B) The dashed line indicates the viscosity of proteins that eluted from the column. The first peak is  $\alpha$ -crystallin ( $\alpha$ A +  $\alpha$ B), the second  $\beta$ H-crystallin, the third  $\beta$ L-crystallin, and the fourth  $\gamma$ -crystallin.

Table 1: Protein Concentrations of Water-Soluble Crystallins Isolated from Wild-Type,  $\alpha$ A-R49C Heterozygous, and  $\alpha$ A-R49C Homozygous Mouse Lenses<sup>a</sup>

lens genotype	protein concentration (mg/mL)
wild type	6.0
$\alpha$ A-R49C heterozygous	4.8
$\alpha$ A-R49C homozygous	1.0

<sup>a</sup> We prepared lens water-soluble proteins by homogenizing mouse lenses in 1 mL of Tris-HCl buffer (pH 7.5) containing 100 mM NaCl, 1 mM DTT, 1 mM EDTA, and 0.1% NaN<sub>3</sub> and centrifuging them at 15000g as described in Materials and Methods. Four lenses were used for wild-type and  $\alpha$ A-R49C heterozygous mice. Because of the significantly smaller size of the lenses of the  $\alpha$ A-R49C homozygous mice, 12 lenses were used. Note the pronounced decrease in the concentration of the soluble proteins in the  $\alpha$ A-R49C homozygous lenses.

$\gamma$ -crystallins (Figure 4B). Surprisingly, the amount of low-molecular mass material in  $\alpha$ A-R49C homozygous lenses was much smaller than expected on the basis of the refractive index (Figure 3A) and UV absorption (280 nm) profiles (Figure 4B), suggesting that the level of epitope interacting with the  $\gamma$ -crystallin antibody was drastically reduced in these lenses. The immunoblot analysis with an  $\alpha$ A-crystallin-specific antibody (Figure 4B) clearly demonstrated that a small amount of  $\alpha$ A-crystallin remained soluble in the  $\alpha$ A-R49C homozygous lenses.  $\alpha$ A-Crystallin is known to bind partially unfolded, denaturing substrates in its role as a

chaperone. To determine the effect of the  $\alpha$ A-R49C mutation on the binding of  $\beta$ - and  $\gamma$ -crystallins to the  $\alpha$ -crystallin fraction, we next analyzed the  $\alpha$ -crystallin fractions from wild-type, heterozygous, and homozygous lenses with antibodies to  $\beta$ - and  $\gamma$ -crystallin. Immunoblot analysis indicated a stable binding of  $\beta$ - and  $\gamma$ -crystallin to the  $\alpha$ -crystallin fraction from the  $\alpha$ A-R49C mutant lenses (Figure 4C). In contrast,  $\beta$ - and  $\gamma$ -crystallin were not associated with  $\alpha$ -crystallin from wild-type lenses. This is a clear demonstration that  $\alpha$ -crystallin is associated with  $\beta$ - and  $\gamma$ -crystallin in the mutant lenses.

The difference between the solubility of the mutant  $\alpha$ A-crystallin in the native state and those of the wild type may be caused by local changes in protein conformation of the mutant  $\alpha$ A-crystallin that expose hydrophobic patches as a result of point mutations. To test this possibility, we compared the surface hydrophobicity of wild-type and mutant  $\alpha$ A-crystallin. The surface hydrophobicity was determined by bis-ANS fluorescence. Bis-ANS, a hydrophobic probe, is nonfluorescent in aqueous solution and becomes fluorescent when bound to the hydrophobic residues on the surface of a molecule (37, 38). Figure 5 shows that the bis-ANS fluorescence increased in direct proportion to the increase in the level of  $\alpha$ A-R49C expression in the  $\alpha$ -crystallin fractions from wild-type,  $\alpha$ A-R49C heterozygous, and  $\alpha$ A-R49C homozygous mouse lenses. The fluorescence intensity

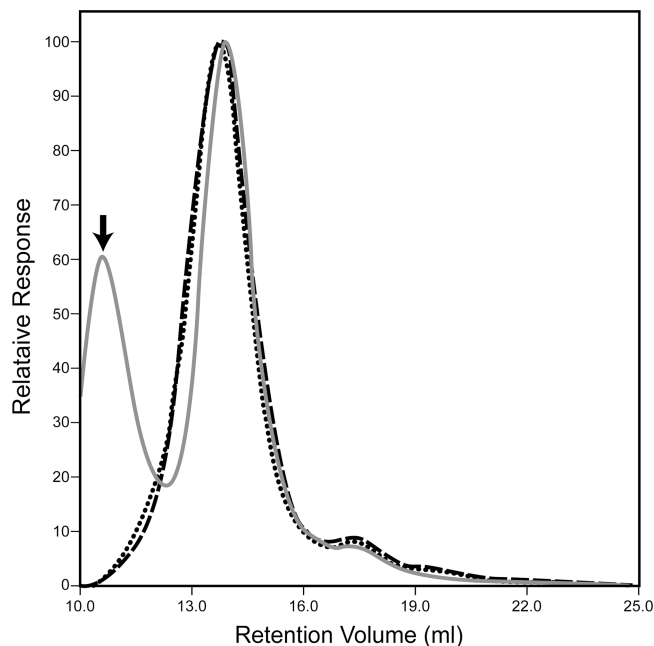


FIGURE 2: Abundance of a high-molecular mass soluble protein species in  $\alpha$ A-R49C homozygous lenses detected by light scattering: wild-type (dashed line),  $\alpha$ A-R49C heterozygous (dotted line), and  $\alpha$ A-R49C homozygous lenses (solid gray line). Note the protein peak in the void volume of the gel permeation chromatography column in  $\alpha$ A-R49C homozygous lens proteins but not in wild-type or  $\alpha$ A-R49C heterozygous proteins.

of bis-ANS in buffer increased 8-fold in the presence of  $\alpha$ -crystallin from wild-type lenses. The bis-ANS fluorescence further increased 1.5- and 2.2-fold over that of the wild type in the presence of  $\alpha$ -crystallin isolated from  $\alpha$ A-R49C heterozygous and  $\alpha$ A-R49C homozygous lenses, respectively.

Previous studies showed that the thermodynamic stability of  $\alpha$ A- and  $\alpha$ B-crystallin can be determined by measuring temperature-induced unfolding and insolubility (28, 39, 40). Therefore, we next compared the thermal stability of the  $\alpha$ -crystallin fraction from wild-type and mutant lenses. The mutant protein was susceptible to heat-induced aggregation at 65 °C within 10 min, whereas the wild-type protein exhibited much lower light scattering (Figure 6). The mutant protein formed light scattering aggregates above 42 °C, whereas the wild-type protein remained clear and stable in solution up to 53 °C (data not shown). This suggested that the mutant protein was sensitive to temperature above 42 °C.

## DISCUSSION

The lenses of hereditary cataract patients in the family described by Mackay et al. (26) with the  $\alpha$ A-R49C mutation develop a “nuclear” cataract at an early age. These patients have one chromosomal copy of normal  $\alpha$ A-crystallin allele and one copy of the mutant allele that produces the  $\alpha$ A-R49C protein. Thus in lens cells of these patients, an  $\alpha$ A-crystallin molecule consists of complexes containing an equal amount of normal and mutant  $\alpha$ A-crystallin subunits. To gain a better understanding of the effect of the mutation in vivo, we have created a knock-in mouse model to genetically recapitulate this cataract-causing mutation in  $\alpha$ A-crystallin using a novel embryonic stem cell-based genetic approach (34). The  $\alpha$ A-R49C heterozygous mice develop anterior and

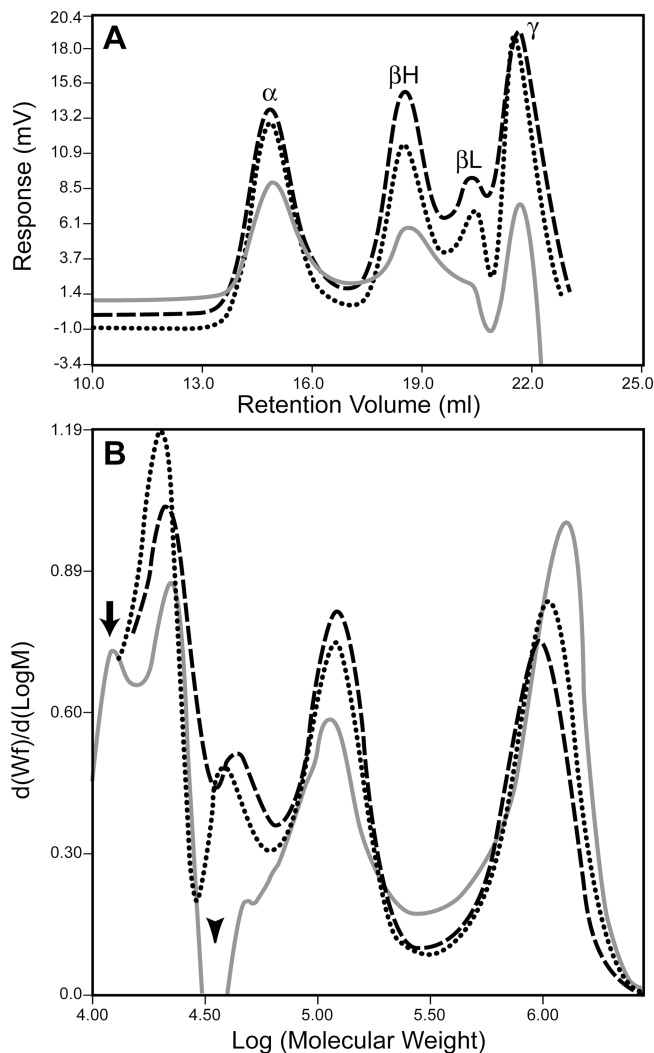


FIGURE 3: Refractive indexes and differential molecular mass distributions of crystallins isolated from wild-type and  $\alpha$ A-R49C mutant lenses. (A) Refractive index profile of crystallins separated by gel permeation chromatography: wild-type (dashed line),  $\alpha$ A-R49C heterozygous (dotted line), and  $\alpha$ A-R49C homozygous lenses (solid gray line). Note the dramatic decrease in the level of  $\beta$ L-crystallin in the soluble fraction of  $\alpha$ A-R49C homozygous lenses. (B) Differential molecular mass distribution of wild-type (dashed line),  $\alpha$ A-R49C heterozygous (dotted line), and  $\alpha$ A-R49C homozygous lenses (solid gray line). Note the diminution in the level of  $\beta$ L-crystallin (60 kDa) in the  $\alpha$ A-R49C homozygous lenses (arrowhead). Also note the increase in the level of a 15 kDa protein in the  $\alpha$ A-R49C homozygous lenses (arrow).

posterior lens changes at eye opening (3 weeks old), and at 4 months of age, these mice also develop a nuclear opacity. The  $\alpha$ A-R49C heterozygous mice have been interbred to generate  $\alpha$ A-R49C homozygous mice. The homozygous mice not only develop cataracts but also demonstrate a small eye phenotype not observed in the heterozygous mice or human patients which are heterozygous for the mutation, although micro-ophthalmia has been reported with another cataract-causing mutation in  $\alpha$ A-crystallin,  $\alpha$ A-R116C (4).

The lenses of  $\alpha$ A-R49C homozygous mice allowed us to assess the effect on protein insolubility in vivo in the absence of any normal  $\alpha$ A-crystallin subunits in this study. We demonstrate that the in vivo effect of  $\alpha$ A-R49C is to make a large proportion of the soluble crystallins insoluble in the homozygous knock-in lenses. Most small heat shock proteins assemble into polydisperse and dynamic oligomers, and their

Table 2: Effect of the  $\alpha$ A-R49C Mutation on Molecular Mass, Intrinsic Viscosity, and Radius of Gyration of Major Crystallin Peaks

	molecular mass (kDa)	intrinsic viscosity (dL/g)	radius of gyration ( $R_g$ ) (nm)
$\alpha$ -crystallin fraction			
wild-type lens	1004	0.065	13.29
$\alpha$ A-R49C heterozygous lens	1061	0.063	13.22
$\alpha$ A-R49C homozygous lens	1150	0.077	14.28
$\beta$ H-crystallin fraction			
wild-type lens	105.2	0.044	5.32
$\alpha$ A-R49C heterozygous lens	114.5	0.046	5.54
$\alpha$ A-R49C homozygous lens	123.0	0.052	5.85
$\beta$ L-crystallin fraction			
wild-type lens	63.1	0.057	5.04
$\alpha$ A-R49C heterozygous lens	65.0	0.043	4.64
$\alpha$ A-R49C homozygous lens	ND <sup>a</sup>	ND <sup>a</sup>	ND <sup>a</sup>
$\gamma$ -crystallin fraction			
wild-type lens	22.6	0.0418	3.24
$\alpha$ A-R49C heterozygous lens	19.2	0.044	3.11
$\alpha$ A-R49C homozygous lens	19.8	0.038	2.80

<sup>a</sup> Not determined.

heterogeneity is enhanced by substrate binding. Investigators have shown that both  $\alpha$ A- and  $\alpha$ B-crystallin form oligomers of different sizes and shapes (41). The oligomeric assembly of mutant  $\alpha$ A-crystallin indicates that oligomers larger than the wild-type protein are formed (40). The cataract-causing R116C mutant of  $\alpha$ A-crystallin forms water-soluble oligomers with a weight-average molecular mass twice as high as that of the wild-type protein (42). Similarly, the G98R  $\alpha$ A-crystallin mutant protein forms highly polydisperse aggregates with an average molecular mass 5-fold higher than that of the normal protein (40). Likewise, cataract-causing mutations in  $\alpha$ B-crystallin also give rise to water-soluble aggregates with average masses 1.5–2-fold higher than that of the wild-type protein (28, 43). Our results with the  $\alpha$ -crystallin fraction isolated from the *in vivo* knock-in lenses showed that the radius of gyration ( $R_g$ ) of the water-soluble  $\alpha$ -crystallin aggregate increased from a value of 13.3 nm in wild-type lenses to 14.3 nm in homozygous lenses. These values are based on intrinsic viscosity measurements, which are generally low for compact proteins. Our software performed the  $R_g$  calculation but did not have the hydrodynamic radius ( $R_h$ ) calculating capability.  $R_g$  values are 30–40% higher than  $R_h$  values. For example, the published  $R_h$  of wild-type lens  $\alpha$ -crystallin is 8–9 nm (40). Nonetheless, the  $R_g$  values reported here are reliable and useful parameters for assessing changes in protein aggregation.

The molecular mass determinations reported here are based on light scattering measurements. The water-soluble  $\alpha$ -crystallin molecular mass increased slightly from 1004 kDa for the wild type to 1061 and 1150 kDa for heterozygous and homozygous lenses, respectively. In contrast to previous studies, however, our results show that the major effect *in vivo* of the  $\alpha$ A-R49C mutation in the homozygous lenses was a drastic reduction in overall protein solubility. These results show that when  $\alpha$ A-R49C starts to become a higher-molecular mass species, it just becomes water-insoluble. The high-molecular mass peak eluting in the void volume of the light scattering profile shows a small amount of high-molecular mass aggregated material in  $\alpha$ A-R49C homozygous lenses which is still water-soluble. The presence of this high-molecular mass soluble protein aggregate in the  $\alpha$ A-R49C homozygous lenses provides direct evidence of the

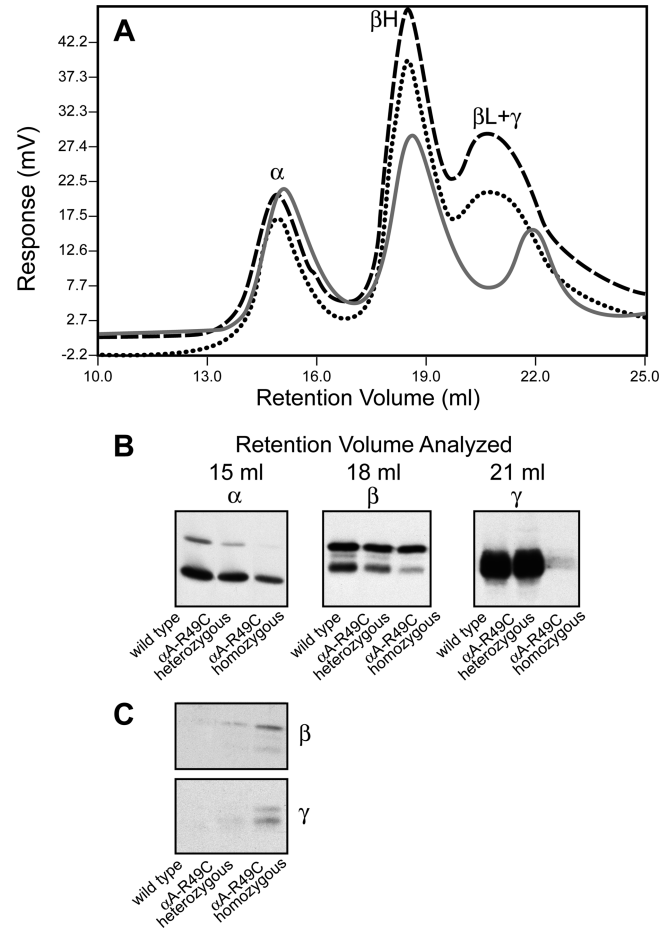


FIGURE 4: UV absorbance and immunoblot analysis of lens protein fractions from wild-type and  $\alpha$ A-R49C mutant lenses. Wild-type lenses (dashed line),  $\alpha$ A-R49C heterozygous lenses (dotted line), and  $\alpha$ A-R49C homozygous lenses (solid gray line). (A) UV absorbance at 280 nm. (B) Immunoblots represent the peak fractions of  $\alpha$ -crystallin,  $\beta$ H-crystallin, and  $\beta$ L- and  $\gamma$ -crystallin obtained from chromatographic separation of wild-type,  $\alpha$ A-R49C heterozygous, and  $\alpha$ A-R49C homozygous lens water-soluble proteins, respectively. Immunoblot analysis of the chromatography peak fractions with antibodies to  $\alpha$ -crystallin, total  $\beta$ -crystallin, and total  $\gamma$ -crystallin was performed. Note the distinct loss of immunoreactivity to  $\gamma$ -crystallin antibody in the  $\alpha$ A-R49C homozygous lens proteins. Note also that the concentration of the water-soluble  $\alpha$ -crystallin fraction ( $\alpha$ A +  $\alpha$ B) was the highest in the wild type and decreased gradually in the  $\alpha$ A-R49C heterozygous and homozygous lenses. (C) Immunoblot analysis of the  $\alpha$ -crystallin fraction of wild-type,  $\alpha$ A-R49C heterozygous, and  $\alpha$ A-R49C homozygous lenses with antibodies to  $\beta$ - and  $\gamma$ -crystallin. Note the gradual increase in  $\beta$ - and  $\gamma$ -crystallin immunoreactivity in the heterozygous and homozygous  $\alpha$ -crystallin fractions. Note also that  $\beta$ - and  $\gamma$ -crystallin immunoreactivity was absent in the wild-type  $\alpha$ -crystallin fraction.

formation of an unstable, intermediate species in the homozygous lenses.

The finding that disruption of the  $\alpha$ A-crystallin N-terminal arginine 49 residue profoundly affects the solubility agrees with the paradigm that sequence divergence in the N-terminal domain of small heat shock proteins is a primary mechanism for regulating the oligomer solubility and degree of order (29, 44, 45). The N-terminal domain of small heat shock proteins is known to be important in recognition of substrates (33, 46). Investigators have suggested that perturbation in the N-terminal region is transmitted to the C-terminal region of the  $\alpha$ -crystallin domain, leading to an

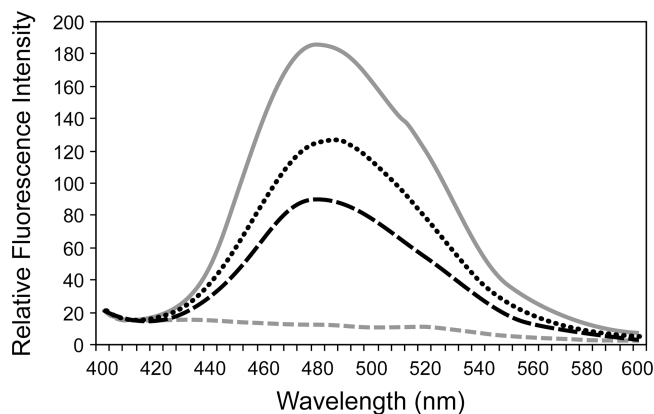


FIGURE 5: Bis-ANS fluorescence in wild-type and  $\alpha$ A-R49C mutant lenses. The fluorescence of bis-ANS ( $5 \mu\text{M}$ ) was measured using an excitation wavelength of 360 nm. The emission was measured from 400 to 600 nm. Emission spectra of bis-ANS in buffer (dashed gray line), a 0.1 mg/mL  $\alpha$ -crystallin fraction from wild-type mouse lenses (black dashed line), an  $\alpha$ -crystallin fraction from  $\alpha$ A-R49C heterozygous mouse lenses (dotted line), and an  $\alpha$ -crystallin fraction from  $\alpha$ A-R49C homozygous mouse lenses (solid gray line). Note the fluorescence emission maximum of bis-ANS at 480 nm upon binding to  $\alpha$ -crystallin. Note also the prominent enhancement in fluorescence intensity of bis-ANS bound to the  $\alpha$ -crystallin fraction isolated from  $\alpha$ A-R49C mutant lenses.

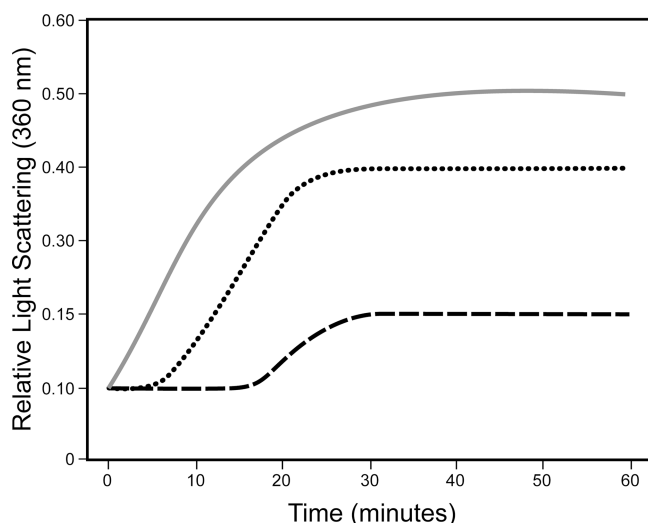


FIGURE 6: Thermal stability of lens proteins from wild-type and  $\alpha$ A-R49C mutant lenses. The thermal stability of the  $\alpha$ -crystallin fraction was determined by the time-dependent change in light scattering as monitored at 360 nm and  $65^\circ\text{C}$ : wild-type (dashed line),  $\alpha$ A-R49C heterozygous (dotted line), and  $\alpha$ A-R49C homozygous (solid gray line). By the 10 min incubation point, the  $\alpha$ -crystallin fraction of the  $\alpha$ A-R49C lenses began to aggregate and precipitate out of solution. In contrast, wild-type  $\alpha$ -crystallin exhibited significantly lower light scattering.

expansion of the structure of Hsp16.5 (32). Previous studies of substrate binding to mutant  $\alpha$ A-crystallin indicated an expansion of the oligomeric assembly, and this was attributed to greater substrate binding and an increase in the insolubility of the substrate-chaperone complex. These mutants also exhibited a higher affinity for their substrates (32). In our  $\alpha$ A-R49C heterozygous and homozygous mutant lenses but not the wild type, the  $\alpha$ -crystallin fraction separated by gel permeation chromatography had increasing amounts of stably bound  $\beta$ - and  $\gamma$ -crystallins, two proteins strongly expressed in lens fiber cells. These results indicate that as  $\alpha$ A-crystallin

starts to bind  $\beta$ - and  $\gamma$ -crystallin, it begins to become insoluble, which corresponds with the phenotype of the cataractous lens. The stably bound  $\beta$ - and  $\gamma$ -crystallin identified in the  $\alpha$ -crystallin fraction are assumed to be in an extensively unfolded state and are recognized by the chaperone protein (32). These interactions are likely to be crucial in determining the ultimate fate of the  $\alpha$ -crystallin oligomer. The data presented in this study can be interpreted by the model in which the aggregate size of mutant  $\alpha$ A-crystallin increases to produce a water-soluble high-molecular mass intermediate species that precipitates out of solution. As lens crystallins exist at a high protein concentration in lens fiber cells, the mechanism described above could be an important factor underlying the human disease phenotype.

The results of this study show that a significant proportion of the  $\alpha$ A-crystallin was insoluble in  $\alpha$ A-R49C homozygous lenses. To understand the mechanism of insolubilization by the  $\alpha$ A-R49C mutation, the hydrophobicity of the  $\alpha$ -crystallin fraction isolated by gel permeation chromatography was measured (Figure 5). Bis-ANS is a sensitive probe that has been shown to bind to a hydrophobic region of the protein (47). Investigators have shown that increasing the temperature increases the level of binding of bis-ANS to  $\alpha$ -crystallin due to the exposure of hydrophobic sites on the protein (48, 49). It has also been found that denaturation and refolding of  $\alpha$ -crystallin enhance the binding of bis-ANS to the protein due to an increase in the level of exposure of hydrophobic sites (47, 48). The gradual enhancement of the fluorescence yield of bis-ANS from wild-type to heterozygous to homozygous  $\alpha$ -crystallin fractions indicates that the hydrophobicity of the protein increases with the  $\alpha$ A-R49C mutation. Interestingly, a hydrophobic sequence from residue 41 to 58 in the related protein  $\alpha$ B-crystallin has been shown to be selective for interactions with fully unfolded substrates (46). Similarly, studies on  $\alpha$ B-crystallin have shown that the D140N mutation associated with hereditary cataracts leads to an increase in hydrophobicity and partial unfolding of the protein (28). In addition, with aging,  $\alpha$ -crystallin undergoes partial unfolding and an increased level of aggregation (14, 50). Solvent exposure of hydrophobic interfaces has been shown to cause a loss of protein solubility (51, 52). A delicate balance between the positions of hydrophobic and charged amino acids can also contribute to the aggregation behavior of proteins (53). Although the increased hydrophobicity of proteins may not always correlate with protein insolubility, it is likely to be one of the factors contributing to protein insolubility of the  $\alpha$ A-R49C mutant lenses. The results of this study suggest that the  $\alpha$ A-R49C mutation exposes hydrophobic sites and leads to stronger bis-ANS binding. The adverse effect of exposure of these hydrophobic patches in the  $\alpha$ A-R49C mutant is that the proteins aggregate at high concentrations present in the lens fiber cells in vivo. The bis-ANS fluorescence enhancement uncovers a change in the protein aggregation dynamics of the  $\alpha$ -crystallin fraction of  $\alpha$ A-R49C mutant lenses.

The most interesting finding in this study is that a minor change in the molecular mass of the  $\alpha$ -crystallin fraction causes a substantial increase in the amount of  $\beta$ - and  $\gamma$ -crystallin associated with the water-soluble fraction of homozygous lenses (Figure 4C). The reduction in the level of  $\beta$ L-crystallin and the disappearance of  $\gamma$ -crystallin from the soluble fraction of  $\alpha$ A-R49C homozygous lenses (Figures



3 and 4) may be explained by the enhanced hydrophobicity of the mutant  $\alpha$ -crystallin in the  $\alpha$ A-R49C homozygous lenses.  $\beta$ L-Crystallin disappeared from the proteins separated by gel permeation chromatography, suggesting that it became insoluble. In 3-week-old knock-in mouse lenses, the degree of interaction between  $\alpha$ A-crystallin and  $\beta$ -crystallin was found to increase in heterozygous lenses by co-immunoprecipitation analysis (34). The loss of the  $\beta$ L-crystallin in homozygous lenses in gel permeation chromatography suggests that the interaction between  $\beta$ L-crystallin and  $\alpha$ A-R49C may not be sufficiently strong to persist during gel permeation chromatography. Alternatively,  $\alpha$ -crystallin may be partly responsible for keeping the  $\beta$ L-crystallin in the soluble phase, and when  $\alpha$ A-crystallin is mutated and becomes insoluble, the solubility of  $\beta$ -crystallin is also diminished. Furthermore, the appearance of the lower-molecular mass peak and the dramatic reduction in the immunoreactivity of  $\gamma$ -crystallin from homozygous lenses suggest a change in the  $\gamma$ -crystallin epitope reacting with the antibody. Future studies will examine whether the presence of wild-type  $\alpha$ -crystallin inhibits the loss of this low-molecular mass  $\gamma$ -crystallin.

The results of our study with  $\alpha$ A-R49C heterozygous lens homogenates suggest that the presence of wild-type  $\alpha$ A-crystallin likely plays a role in buffering the impact of the  $\alpha$ A-R49C mutant protein by diluting its deleterious effect on long-term protein stability. The complete loss of functional  $\alpha$ A-crystallin in homozygous lenses enhances the binding of the substrate to unfolding states, leading to an increased level of insolubilization. These results clearly demonstrate that the biological effect of the  $\alpha$ A-R49C mutation is to increase the level of aggregation of the water-soluble  $\alpha$ -crystallin, ultimately causing insolubilization and lens opacification.

The  $\alpha$ A-R49C mutation lies outside the conserved  $\alpha$ -crystallin domain. Investigators have examined the properties of several arginine mutants in the C-terminal domain of  $\alpha$ A-crystallin in vitro (42, 54, 55). The N-terminal mutant  $\alpha$ A-crystallin with the arginine 49 to alanine (R49A) mutation had a molar mass significantly higher than that of the wild-type protein (56). The  $\alpha$ A-R49C mutant proteins isolated from the heterozygous and homozygous lenses had slightly greater radii of gyration. While most of the  $\alpha$ -crystallin from homozygous knock-in lenses becomes water-insoluble, a small amount of  $\alpha$ A-crystallin could be detected in the soluble fraction. As the lens fiber cells express  $\alpha$ A- and  $\alpha$ B-crystallin in a 3:1 stoichiometry, the fact that even in the absence of any wild-type  $\alpha$ A-crystallin in  $\alpha$ A-R49C homozygous lenses, a small amount of  $\alpha$ A-crystallin does remain water-soluble indicates a protective role of  $\alpha$ B-crystallin. Other studies indicate that the  $\alpha$ A-crystallin R54H mutation, which also lies outside the conserved  $\alpha$ -crystallin domain, produces high-molecular mass aggregates and recessive cataracts in mice (57). It is also well established that the molecular mass of  $\alpha$ -crystallin increases with aging and cataracts, and a water-soluble high-molecular mass  $\alpha$ -crystallin has been reported in aged human lenses (50, 58). It should be noted that this study characterizes only the water-soluble proteins of the lens, which is not one and the same as lens transparency (14). A clear adult human lens has a significant amount of water-insoluble material. Because of the differences in water solubility observed in this study

(Table 1), the percentage of total lens proteins being analyzed in the water-soluble protein fraction probably represents a significant proportion (80–90%, based on studies in the literature) of the total lens protein in wild-type lenses, but a markedly smaller fraction in the  $\alpha$ A-R49C homozygous lenses, with heterozygous lenses being intermediate between these two values.

In summary, using a mouse model for human hereditary cataracts, the results of this study provide key insights into the mechanism of protein insolubilization by a point mutation in  $\alpha$ A-crystallin, show clear evidence that  $\beta$ - and  $\gamma$ -crystallin stably bind  $\alpha$ -crystallin in mutant lenses, reveal an increase in the surface hydrophobicity of the mutant protein, and demonstrate the existence of a water-soluble high-molecular mass intermediate in the cataractous lenses. These data suggest that  $\alpha$ A-R49C has a tendency to become unstable and bind more unfolded substrate proteins. Expression of both wild-type and mutant  $\alpha$ A-crystallin in the heterozygous lenses reduces the level of formation of proteins containing exposed hydrophobic regions, reducing the rate of their transition into high-molecular mass water-insoluble species. Although the molecular mass of the water-soluble  $\alpha$ -crystallin fraction was not very different among the three different genotypes studied, the binding of  $\beta$ - and  $\gamma$ -crystallins was different, probably because of the differences in hydrophobicity of  $\alpha$ -crystallin. Further studies of  $\alpha$ -crystallin with neutron scattering in solution are in progress to determine the molecular structure of the  $\alpha$ A-R49C protein.

## REFERENCES

1. Van Montfort, R., Slingsby, C., and Vierling, E. (2001) Structure and function of the small heat shock protein/ $\alpha$ -crystallin family of molecular chaperones. *Adv. Protein Chem.* 59, 105–156.
2. de Jong, W. W., Caspers, G. J., and Leunissen, J. A. (1998) Genealogy of the  $\alpha$ -crystallin-small heat-shock protein superfamily. *Int. J. Biol. Macromol.* 22, 151–162.
3. Andley, U. P. (2007) Crystallins in the eye: Function and pathology. *Prog. Retinal Eye Res.* 26, 78–98.
4. Litt, M., Kramer, P., LaMorticella, D. M., Murphey, W., Lovrien, E. W., and Weleber, R. G. (1998) Autosomal dominant congenital cataract associated with a missense mutation in the human  $\alpha$  crystallin gene CRYAA. *Hum. Mol. Genet.* 7, 471–474.
5. Sax, C. M., and Piatigorsky, J. (1994) Expression of the  $\alpha$ -crystallin/small heat-shock protein/molecular chaperone genes in the lens and other tissues. *Adv. Enzymol. Relat. Areas Mol. Biol.* 69, 155–201.
6. Andley, U. P. (2006) Crystallins and hereditary cataracts: Molecular mechanisms and potential for therapy. *Expert Rev. Mol. Med.* 8, 1–19.
7. Kappe, G., Franck, E., Verschuure, P., Boelens, W. C., Leunissen, J. A., and de Jong, W. W. (2003) The human genome encodes 10  $\alpha$ -crystallin-related small heat shock proteins: HspB1–10. *Cell Stress Chaperones* 8, 53–61.
8. Horwitz, J. (1992)  $\alpha$ -Crystallin can function as a molecular chaperone. *Proc. Natl. Acad. Sci. U.S.A.* 89, 10449–10453.
9. Sun, T. X., Das, B. K., and Liang, J. J. (1997) Conformational and functional differences between recombinant human lens  $\alpha$ A- and  $\alpha$ B-crystallin. *J. Biol. Chem.* 272, 6220–6225.
10. Andley, U. P., Song, Z., Wawrousek, E. F., and Bassnett, S. (1998) The molecular chaperone  $\alpha$ A-crystallin enhances lens epithelial cell growth and resistance to UVA stress. *J. Biol. Chem.* 273, 31252–31261.
11. Andley, U. P., Song, Z., Wawrousek, E. F., Brady, J. P., Bassnett, S., and Fleming, T. P. (2001) Lens epithelial cells derived from  $\alpha$ B-crystallin knockout mice demonstrate hyperproliferation and genomic instability. *FASEB J.* 15, 221–229.
12. Brady, J. P., Garland, D., Douglas-Tabor, Y., Robison, W. G., Jr., Groome, A., and Wawrousek, E. F. (1997) Targeted disruption of the mouse  $\alpha$ A-crystallin gene induces cataract and cytoplasmic



- inclusion bodies containing the small heat shock protein  $\alpha$ B-crystallin. *Proc. Natl. Acad. Sci. U.S.A.* 94, 884–889.
13. Brady, J. P., Garland, D. L., Green, D. E., Tamm, E. R., Giblin, F. J., and Wawrousek, E. F. (2001)  $\alpha$ B-Crystallin in lens development and muscle integrity: A gene knockout approach. *Invest. Ophthalmol. Visual Sci.* 42, 2924–2934.
  14. Bloemendal, H., de Jong, W., Jaenicke, R., Lubsen, N. H., Slingsby, C., and Tardieu, A. (2004) Ageing and vision: Structure, stability and function of lens crystallins. *Prog. Biophys. Mol. Biol.* 86, 407–485.
  15. Hejtmancik, F., and Piatigorsky, J. (2000) *Lens proteins and their molecular biology*, 2nd ed., Vol. 2, W. B. Saunders, Philadelphia.
  16. Lampi, K. J., Shih, M., Ueda, Y., Shearer, T. R., and David, L. L. (2002) Lens proteomics: Analysis of rat crystallin sequences and two-dimensional electrophoresis map. *Invest. Ophthalmol. Visual Sci.* 43, 216–224.
  17. Jaenicke, R., and Slingsby, C. (2001) Lens crystallins and their microbial homologs: Structure, stability, and function. *Crit. Rev. Biochem. Mol. Biol.* 36, 435–499.
  18. Bettelheim, F. A. (2004) Light scattering in lens research: An essay on accomplishments and promises. *Exp. Eye Res.* 79, 747–752.
  19. Ponce, A., Sorensen, C., and Takemoto, L. (2006) Role of short-range protein interactions in lens opacifications. *Mol. Vision* 12, 879–884.
  20. Benedek, G. B., Chylack, L. T., Jr., Libondi, T., Magnante, P., and Pennett, M. (1987) Quantitative detection of the molecular changes associated with early cataractogenesis in the living human lens using quasielastic light scattering. *Curr. Eye Res.* 6, 1421–1432.
  21. Thurston, G. M., Hayden, D. L., Burrows, P., Clark, J. I., Taret, V. G., Kandel, J., Courogen, M., Peetermans, J. A., Bowen, M. S., Miller, D., Sullivan, K. M., Storb, R., Stern, H., and Benedek, G. B. (1997) Quasielastic light scattering study of the living human lens as a function of age. *Curr. Eye Res.* 16, 197–207.
  22. Pande, A., Annunziata, O., Asherie, N., Ogun, O., Benedek, G. B., and Pande, J. (2005) Decrease in protein solubility and cataract formation caused by the Pro23 to Thr mutation in human  $\gamma$ D-crystallin. *Biochemistry* 44, 2491–2500.
  23. Pande, A., Pande, J., Asherie, N., Lomakin, A., Ogun, O., King, J., and Benedek, G. B. (2001) Crystal cataracts: Human genetic cataract caused by protein crystallization. *Proc. Natl. Acad. Sci. U.S.A.* 98, 6116–6120.
  24. Pande, A., Pande, J., Asherie, N., Lomakin, A., Ogun, O., King, J. A., Lubsen, N. H., Walton, D., and Benedek, G. B. (2000) Molecular basis of a progressive juvenile-onset hereditary cataract. *Proc. Natl. Acad. Sci. U.S.A.* 97, 1993–1998.
  25. Vicart, P., Caron, A., Guicheney, P., Li, Z., Prevost, M. C., Faure, A., Chateau, D., Chapon, F., Tome, F., Dupret, J. M., Paulin, D., and Fardeau, M. (1998) A missense mutation in the  $\alpha$ B-crystallin chaperone gene causes a desmin-related myopathy. *Nat. Genet.* 20, 92–95.
  26. Mackay, D. S., Andley, U. P., and Shiels, A. (2003) Cell death triggered by a novel mutation in the  $\alpha$ A-crystallin gene underlies autosomal dominant cataract linked to chromosome 21q. *Eur. J. Hum. Genet.* 11, 784–793.
  27. Santhiya, S. T., Soker, T., Klopp, N., Illig, T., Prakash, M. V., Selvaraj, B., Gopinath, P. M., and Graw, J. (2006) Identification of a novel, putative cataract-causing allele in CRYAA (G98R) in an Indian family. *Mol. Vision* 12, 768–773.
  28. Liu, Y., Zhang, X., Luo, L., Wu, M., Zeng, R., Cheng, G., Hu, B., Liu, B., Liang, J. J., and Shang, F. (2006) A Novel  $\alpha$ B-Crystallin Mutation Associated with Autosomal Dominant Congenital Lamellar Cataract. *Invest. Ophthalmol. Visual Sci.* 47, 1069–1075.
  29. Basha, E., Friedrich, K. L., and Vierling, E. (2006) The N-terminal arm of small heat shock proteins is important for both chaperone activity and substrate specificity. *J. Biol. Chem.* 281, 39943–39952.
  30. Giese, K. C., Basha, E., Catague, B. Y., and Vierling, E. (2005) Evidence for an essential function of the N terminus of a small heat shock protein in vivo, independent of in vitro chaperone activity. *Proc. Natl. Acad. Sci. U.S.A.* 102, 18896–18901.
  31. Ghosh, J. G., Estrada, M. R., Houck, S. A., and Clark, J. I. (2006) The function of the  $\beta$ 3 interactive domain in the small heat shock protein and molecular chaperone, human  $\alpha$ B-crystallin. *Cell Stress Chaperones* 11, 187–197.
  32. Koteiche, H. A., and McHaourab, H. S. (2006) Mechanism of a hereditary cataract phenotype. Mutations in  $\alpha$ A-crystallin activate substrate binding. *J. Biol. Chem.* 281, 14273–14279.
  33. Shi, J., Koteiche, H. A., McHaourab, H. S., and Stewart, P. L. (2006) Cryoelectron microscopy and EPR analysis of engineered symmetric and polydisperse Hsp16.5 assemblies reveals determinants of polydispersity and substrate binding. *J. Biol. Chem.* 281, 40420–40428.
  34. Xi, J. H., Bai, F., Gross, J., Townsend, R. R., Menko, A. S., and Andley, U. P. (2008) Mechanism of small heat shock protein function in vivo: A knockin mouse model demonstrates that the R49C mutation in  $\alpha$ A-crystallin enhances protein insolubility and cell death. *J. Biol. Chem.* 283, 5801–5814.
  35. Andley, U. P., Mathur, S., Griest, T. A., and Petrash, J. M. (1996) Cloning, expression, and chaperone-like activity of human  $\alpha$ A-crystallin. *J. Biol. Chem.* 271, 31973–31980.
  36. Fleming, T. P., Song, Z., and Andley, U. P. (1998) Expression of growth control and differentiation genes in human lens epithelial cells with extended life span. *Invest. Ophthalmol. Visual Sci.* 39, 1387–1398.
  37. Liang, J. J., and Fu, L. (2002) Decreased subunit exchange of heat-treated lens  $\alpha$ A-crystallin. *Biochem. Biophys. Res. Commun.* 293, 7–12.
  38. Liang, J. J., Sun, T. X., and Akhtar, N. J. (2000) Heat-induced conformational change of human lens recombinant  $\alpha$ A- and  $\alpha$ B-crystallins. *Mol. Vision* 6, 10–14.
  39. Sun, T. X., Akhtar, N. J., and Liang, J. J. (1999) Thermodynamic stability of human lens recombinant  $\alpha$ A- and  $\alpha$ B-crystallins. *J. Biol. Chem.* 274, 34067–34071.
  40. Murugesan, R., Santhoshkumar, P., and Sharma, K. K. (2007) Cataract-causing  $\alpha$ AG98R mutant shows substrate-dependent chaperone activity. *Mol. Vision* 13, 2301–2309.
  41. Haley, D. A., Bova, M. P., Huang, Q. L., McHaourab, H. S., and Stewart, P. L. (2000) Small heat-shock protein structures reveal a continuum from symmetric to variable assemblies. *J. Mol. Biol.* 298, 261–272.
  42. Shroff, N. P., Cherian-Shaw, M., Bera, S., and Abraham, E. C. (2000) Mutation of R116C results in highly oligomerized  $\alpha$ A-crystallin with modified structure and defective chaperone-like function. *Biochemistry* 39, 1420–1426.
  43. Bova, M. P., Yaron, O., Huang, Q., Ding, L., Haley, D. A., Stewart, P. L., and Horwitz, J. (1999) Mutation R120G in  $\alpha$ B-crystallin, which is linked to a desmin-related myopathy, results in an irregular structure and defective chaperone-like function. *Proc. Natl. Acad. Sci. U.S.A.* 96, 6137–6142.
  44. Bova, M. P., McHaourab, H. S., Han, Y., and Fung, B. K. (2000) Subunit exchange of small heat shock proteins. Analysis of oligomer formation of  $\alpha$ A-crystallin and Hsp27 by fluorescence resonance energy transfer and site-directed truncations. *J. Biol. Chem.* 275, 1035–1042.
  45. Berengian, A. R., Parfenova, M., and McHaourab, H. S. (1999) Site-directed spin labeling study of subunit interactions in the  $\alpha$ -crystallin domain of small heat-shock proteins. Comparison of the oligomer symmetry in  $\alpha$ A-crystallin, HSP 27, and HSP 16.3. *J. Biol. Chem.* 274, 6305–6314.
  46. Ghosh, J. G., Shenoy, A. K., Jr., and Clark, J. I. (2006) N- and C-Terminal motifs in human  $\alpha$ B-crystallin play an important role in the recognition, selection, and solubilization of substrates. *Biochemistry* 45, 13847–13854.
  47. Sharma, K. K., Kaur, H., Kumar, G. S., and Kester, K. (1998) Interaction of 1,1'-bi(4-anilino)naphthalene-5,5'-disulfonic acid with  $\alpha$ -crystallin. *J. Biol. Chem.* 273, 8965–8970.
  48. Das, B. K., and Liang, J. J. (1997) Detection and characterization of  $\alpha$ -crystallin intermediate with maximal chaperone-like activity. *Biochem. Biophys. Res. Commun.* 236, 370–374.
  49. Das, K. P., and Surewicz, W. K. (1995) Temperature-induced exposure of hydrophobic surfaces and its effect on the chaperone activity of  $\alpha$ -crystallin. *FEBS Lett.* 369, 321–325.
  50. Liang, J. N. (1987) Fluorescence study of the effects of aging and diabetes mellitus on human lens  $\alpha$ -crystallin. *Curr. Eye Res.* 6, 351–355.
  51. Norledge, B. V., Mayr, E. M., Glockshuber, R., Bateman, O. A., Slingsby, C., Jaenicke, R., and Driessen, H. P. (1996) The X-ray structures of two mutant crystallin domains shed light on the evolution of multi-domain proteins. *Nat. Struct. Biol.* 3, 267–274.
  52. Pande, A., Zhang, J., Shekhtman, A., and Pande, J. (2008) *Invest. Ophthalmol. Visual Sci. Suppl.*, 284.
  53. Rivers, R. C., Kumita, J. R., Tartaglia, G. G., Dedmon, M. M., Pawar, A., Vendruscolo, M., Dobson, C. M., and Christodoulou, J. (2008) Molecular determinants of the aggregation behavior of  $\alpha$ - and  $\beta$ -synuclein. *Protein Sci.* 17, 887–898.
  54. Andley, U. P., Patel, H. C., and Xi, J. H. (2002) The R116C mutation in  $\alpha$ A-crystallin diminishes its protective ability against

- stress-induced lens epithelial cell apoptosis. *J. Biol. Chem.* 277, 10178–10186.
55. Brown, Z., Ponce, A., Lampi, K., Hancock, L., and Takemoto, L. (2007) Differential binding of mutant (R116C) and wildtype  $\alpha$ A-crystallin to actin. *Curr. Eye Res.* 32, 1051–1054.
56. Biswas, A., Miller, A., Oya-Ito, T., Santhoshkumar, P., Bhat, M., and Nagaraj, R. H. (2006) Effect of site-directed mutagenesis of methylglyoxal-modifiable arginine residues on the structure and chaperone function of human  $\alpha$ A-crystallin. *Biochemistry* 45, 4569–4577.
57. Xia, C. H., Liu, H., Chang, B., Cheng, C., Cheung, D., Wang, M., Huang, Q., Horwitz, J., and Gong, X. (2006) Arginine 54 and Tyrosine 118 residues of  $\alpha$ A-crystallin are crucial for lens formation and transparency. *Invest. Ophthalmol. Visual Sci.* 47, 3004–3010.
58. Liang, J. N., Andley, U. P., and Chylack, L. T., Jr. (1985) Spectroscopic studies on human lens crystallins. *Biochim. Biophys. Acta* 832, 197–203.

BI800594T